Feasibility of anisotropic inversion based on P-wave travel–time curves

Petr Bulant
Department of Geophysics, Faculty of Mathematics and Physics, Charles University in Prague, Ke Karlovu 3, 121 16 Praha 2, Czech Republic,
http://sw3d.cz/staff/bulant.htm

Summary

Obtaining a very basic information about the depth dependence of the seismic velocity in a geological structure, we construct several different velocity models suitable for ray tracing. We then calculate travel times to the set of surface profiles in all the constructed models, simulating numerically a surface seismic refraction measurement. We then study the effects of the different velocity models on the calculated travel–time curves.

We examine effects of smooth model versus model with a structural interface, effects of vertical cracks in the deeper part of the model, effects of VTI anisotropy, and effects of low velocity channels in the lower part of the models.

Keywords

Ray tracing, velocity model, anisotropy, vertical cracks, travel–time curve.

1. Introduction

This study is devoted to numerical forward modelling of refracted P-wave travel–time curves (i.e. surface arrival times plotted in dependence on the distance from the surface source point) in different velocity models. The study aims to illustrate how the different details in the velocity models influence the travel–time curves.

We assume that we have a basic information about a real structure, for example from a sonic measurement in a well, and we plan a surface seismic refraction measurement. We thus construct several velocity models which are all derived from the measured well log, but contain different details in the deeper part of the model. The models we construct in the way that they are suitable for ray tracing. We then assume a surface source of seismic waves and calculate refracted P-wave travel–time curves along several profiles at the surface of the models, and we show how the different subsurface structures influence the resulting travel–time curves, which could help us in designing the surface seismic refraction measurement.

Seismic Waves in Complex 3–D Structures, **26** (2016), 103–122 (ISSN 2336–3827, online at http://sw3d.cz)

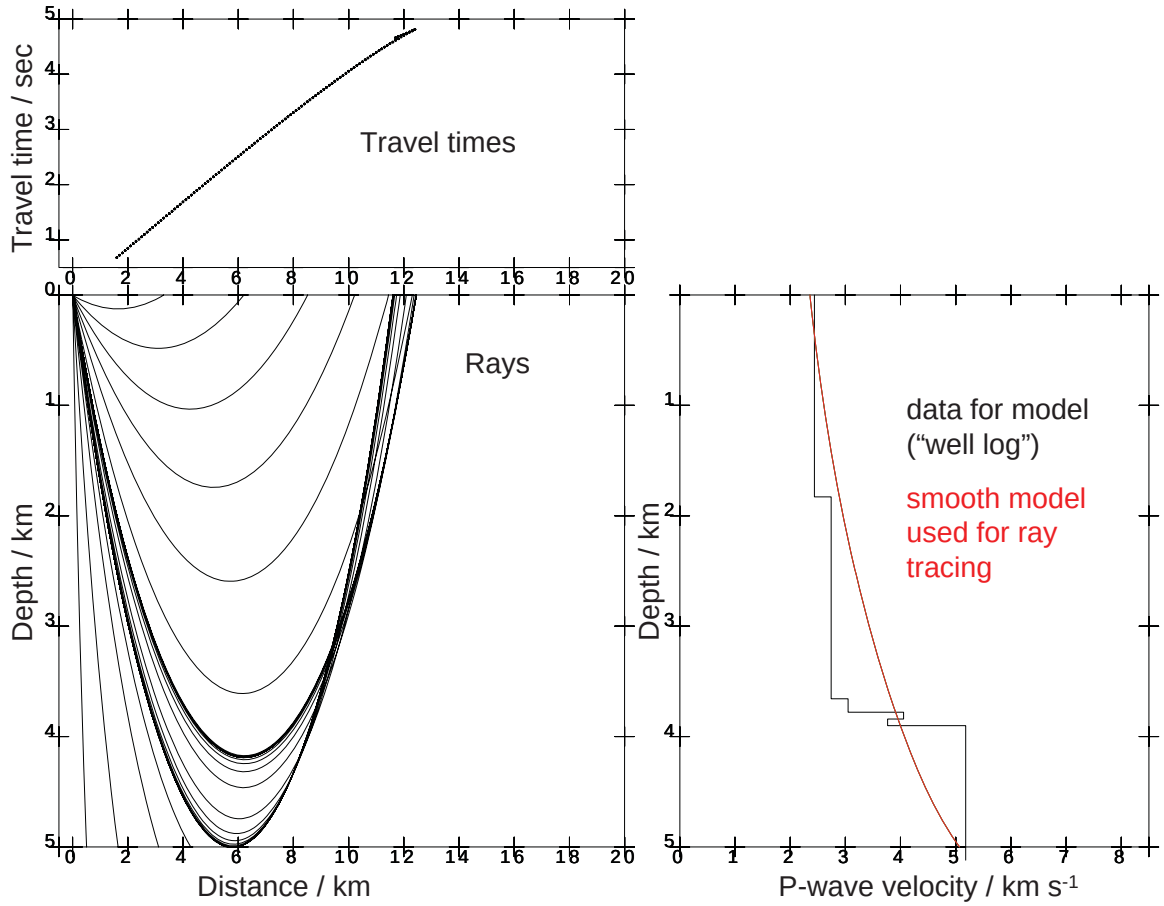

Figure 1: *Bottom right:* the given P–wave velocity used as input data ("well log") for construction of various versions of velocity model (black curve) and smooth P-wave isotropic velocity model number 1 (red curve). *Bottom left:* P-wave rays traced in the $x_1 - x_3$ plane in the isotropic model 1. *Top left:* P-wave travel–time curve (arrival times of the P-wave rays at the surface of the model along the x_1 direction).

2. Travel–time curves in the individual velocity models

Assume that the only information we have about the structure is a 1-D P-wave velocity measurement ("well log"), see the black line in a right bottom panel in Figure 1. The "well log" shows a layer with smaller velocity gradient in the depths up to 3.7 km, then some transition zone in the depths from 3.7 to 4 km, and then a layer with higher velocity below the 4 km depth. Assume that we have also an information that the lower layer may contain vertical cracks and thus may be anisotropic. Based on the available information we construct several different velocity models suitable for ray tracing, and we examine how the different models influence the travel–time curves. We are interested in the differences between a smooth one-block model and a model containing structural interface in the depth of 3.8 km, in the differences between isotropic models and models with anisotropic lower layer, and in the effects caused by a possible low-velocity channel in the lower part of the model.

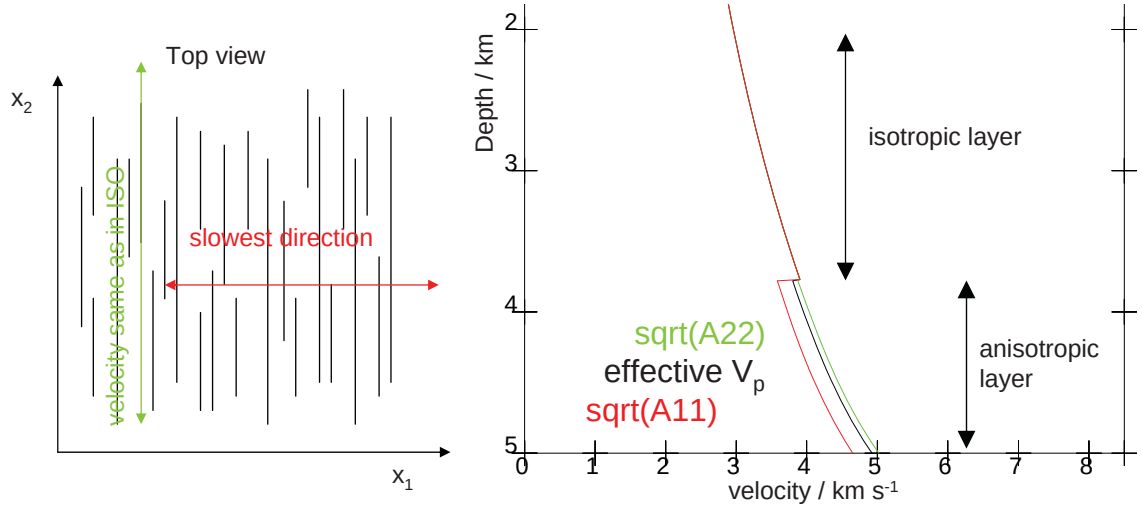

Figure 2: *Left:* a sketch of cracks (thin black lines) inducing the anisotropy in the lower layer of the anisotropic models. The cracks are parallel to the $x_2 - x_3$ plane, which slows down the seismic waves in the x_1 direction, while the velocity in the $x_2 - x_3$ plane remains unchanged - the medium is TI with horizontal axis of symmetry parallel to the x_1 direction. *Right:* illustration of the resulting depth dependence of the stiffness parameters A_{11} and A_{22} in the anisotropic models.

2.1 Smooth one-block model and effects of vertical cracks in the deeper part of the structure

First model we construct is the simplest one, consisting of a single block with P-wave velocity smoothly increasing with the depth. We construct this model by fitting the velocities in the "well log" while simultaneously minimizing the Sobolev norm of the model, refer to Bulant (2002). We call this model "isotropic model 1", see the red line in a right bottom panel in Figure 1. In the constructed model we perform controlled initial–value ray tracing from a source at the surface of the model followed by interpolation of the travel times to the surface profile of receivers according to Bulant & Klimeš (1999) and display the travel–time curve, see Figure 1.

Next we would like to investigate the effects of possible vertical cracks contained in the lower part of the model. We introduce a structural interface in the depth of 3.8 km, and assume that the lower part of the model contains vertical cracks parallel to the $x_2 - x_3$ plane. We calculate the stiffness tensor of the medium using the theory of Schoenberk & Sayers (1995) in the description by Grechka (2009). The vertical cracks parallel to the $x_2 - x_3$ plane slow down the waves propagating in the x_1 direction, while the propagation of the waves in the $x_2 - x_3$ plane is not affected. The resulting medium is thus transversally isotropic (TI) with horizontal axis of symmetry parallel to the x_1 direction, see Figure 2. We construct three versions of anisotropic models differing in the degree of anisotropy. Anisotropic model 1 contains 0.1% of anisotropy, anisotropic model 2 2.8%, and anisotropic model 3 7.5% of anisotropy. See Figures 3 and 4 showing the parameters of the models and their effects on the ray paths and on the travel–time curves calculated along the x_1 axis. We can see that the cracks slow down the rays propagating through the anisotropic layer in the x_1 direction, and cause travel-time delay in the corresponding part of the travel–time curve. The effects are almost invisible in anisotropic model 1, noticeable in anisotropic model 2, and well visible in anisotropic model 3.

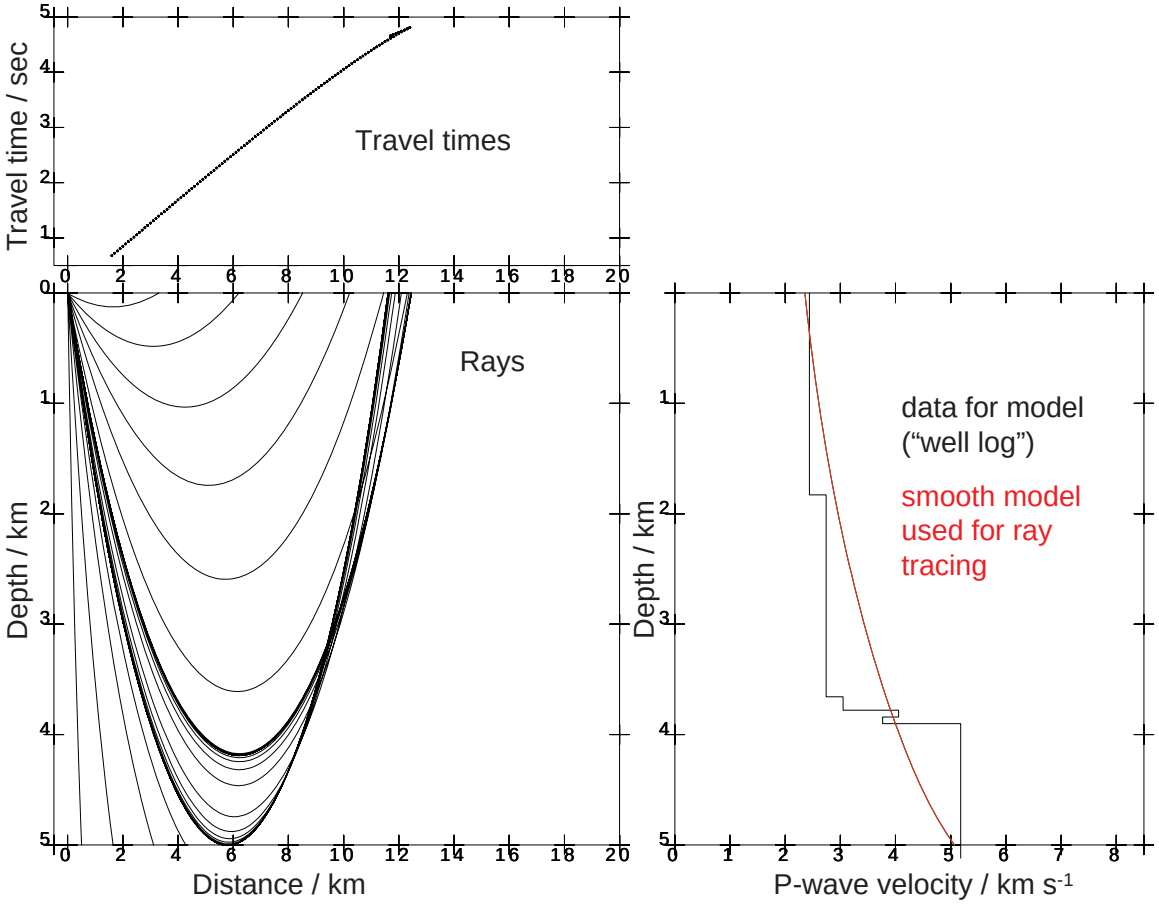

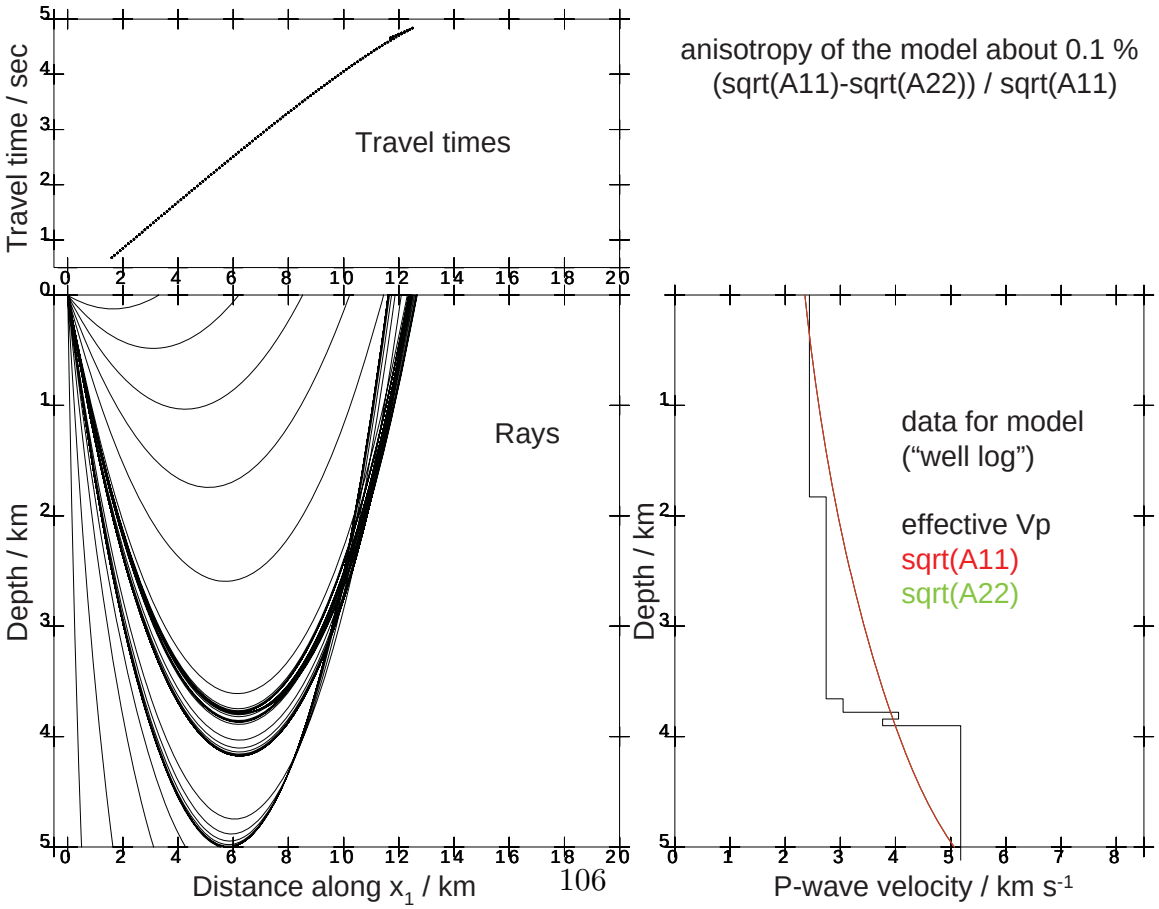

Figure 3: *Top:* isotropic velocity model 1 (repeated Figure 1 shown here for more comfortable comparison with anisotropic models). *Bottom:* anisotropic model 1.

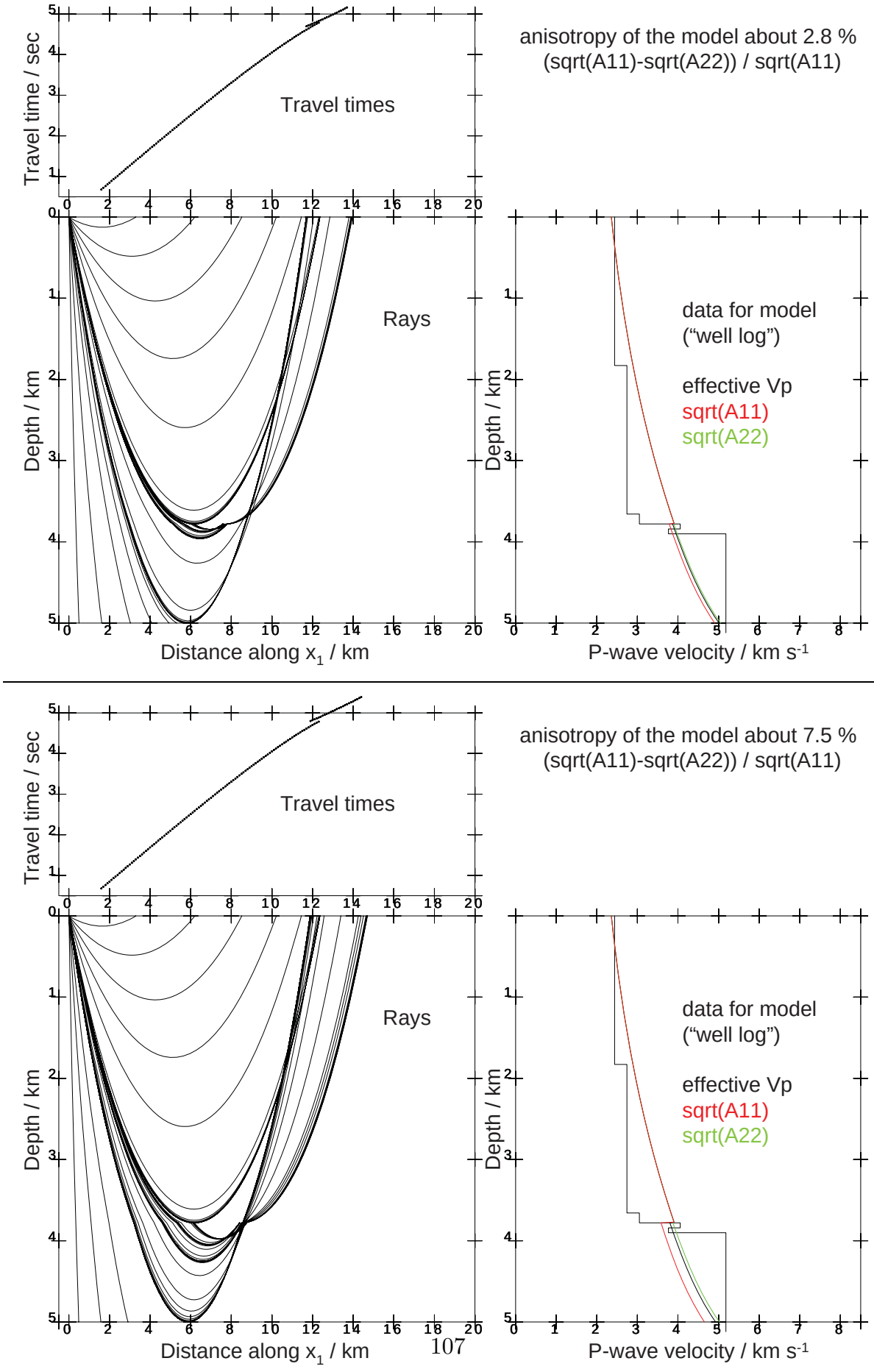

Figure 4: *Top:* anisotropic model 2. *Bottom:* anisotropic model 3.

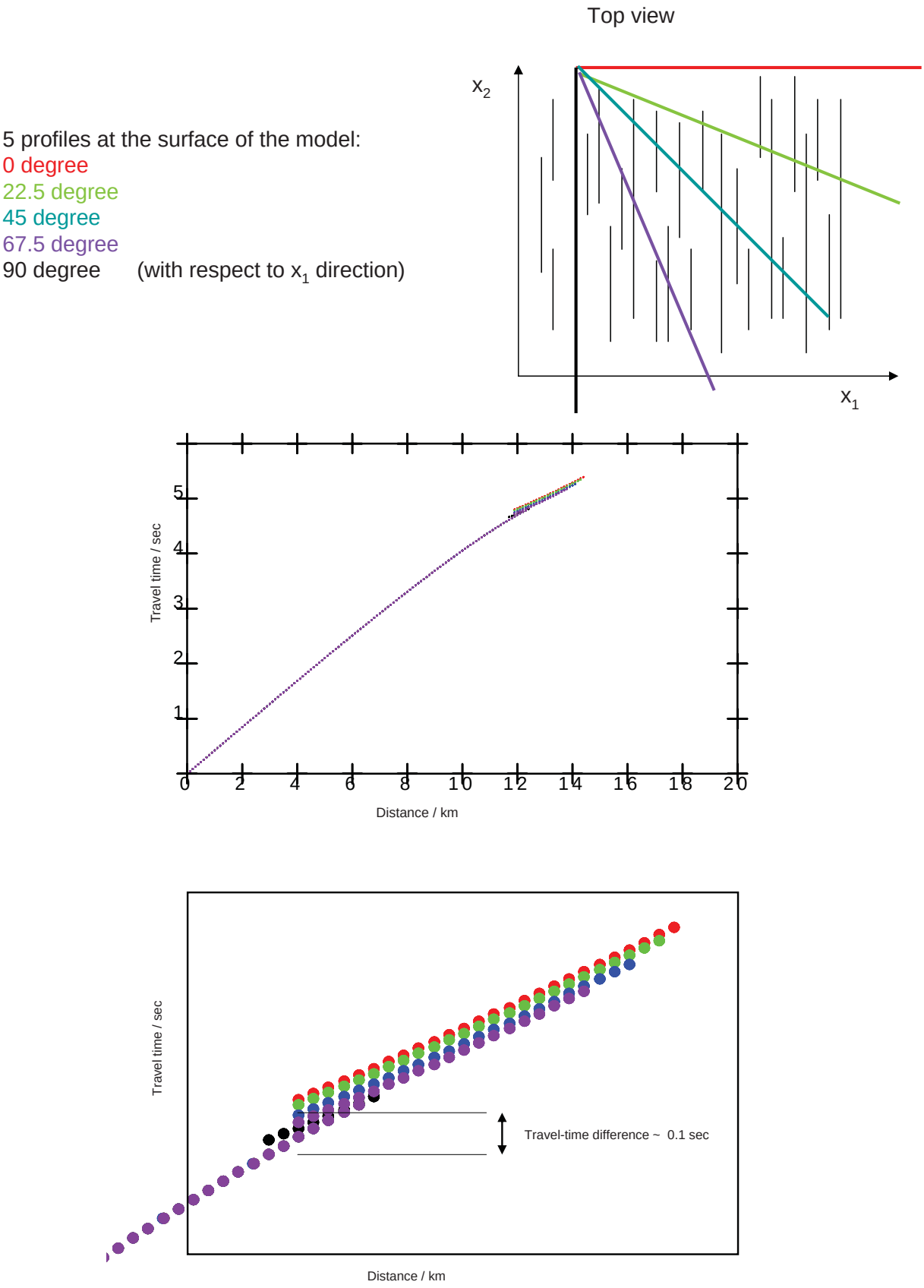

Figure 5: *Top:* a sketch of 5 profiles at the surface of the model. The common origin of the profiles coincides with the source point. *Middle:* travel–time curves along the profiles in anisotropic model 3. *Bottom:* a detail of the travel–time curves.

As a next experiment we calculate travel–time curves in anisotropic model 3 for 5 surface profiles. The profiles originate in the seismic source point and they have different orientation, see Figure 5. Not surprisingly, we see that the slowest are the arrival times along the profile in the x_1 direction, while the profiles in the other directions are less affected, and the profile in the x_2 direction has the same travel times as in the isotropic model 1.

2.2 Models with vertical velocity discontinuity

As can be seen from Figure 1, the "well log" display a high increase in the velocity in the depths from 3.7 to 4 km, and it is not easy to decide whether the isotropic smooth model used for ray tracing should be one-block or whether it should contain a structural interface. In order to examine both variants, we construct the isotropic model 2 containing the structural interface at 3.8 km, see the top panel in Figure 6. We can see that introducing the interface results in lower velocity gradient in the upper layer, which affects the shape of the travel–time curve.

Similarly as anisotropic model 3, we construct anisotropic model 4, which is derived from isotropic model 2, and its lower layer contains again vertical cracks oriented in the $x_2 - x_3$ plane. The anisotropy of anisotropic model 4 is approximately 8.1%, see the lower panel in Figure 6. The anisotropy again slows down the rays propagating in the x_1 direction, see Figure 7.

2.3 Models with inclined structural interface

The observation of the effects of the anisotropic models on the travel–time curves (Figures 5 and 7) raised the question whether these effects can be distinguished from the effects caused by possible inclination of the structural interface. To answer this question we have constructed two alternative versions of isotropic model 2 - one with the interface inclined towards the source, and one with interface declined away of the source. Figure 9 shows the velocity sections, rays traced in the $x_1 - x_3$ plane, and the travel–time curves along the 5 profiles in the models with inclined and declined interface. When compared to Figure 8, Figure 9 demonstrates that the effects of declined interface are very similar to the effects of vertical cracks, while inclined interface has an opposite effect - it speeds up the travel times along the rays propagating in the x_1 direction and shifts the travel–time curves in the opposite way than the declined interface.

When we add the anisotropy caused by the vertical cracks to the lower layer of the models with inclined and declined interface, the effects of dipping interfaces are combined with the effects of anisotropy. Figure 10 shows that in the case of declined interface the effects sum up, while in the model with inclined interface the effects act against each other.

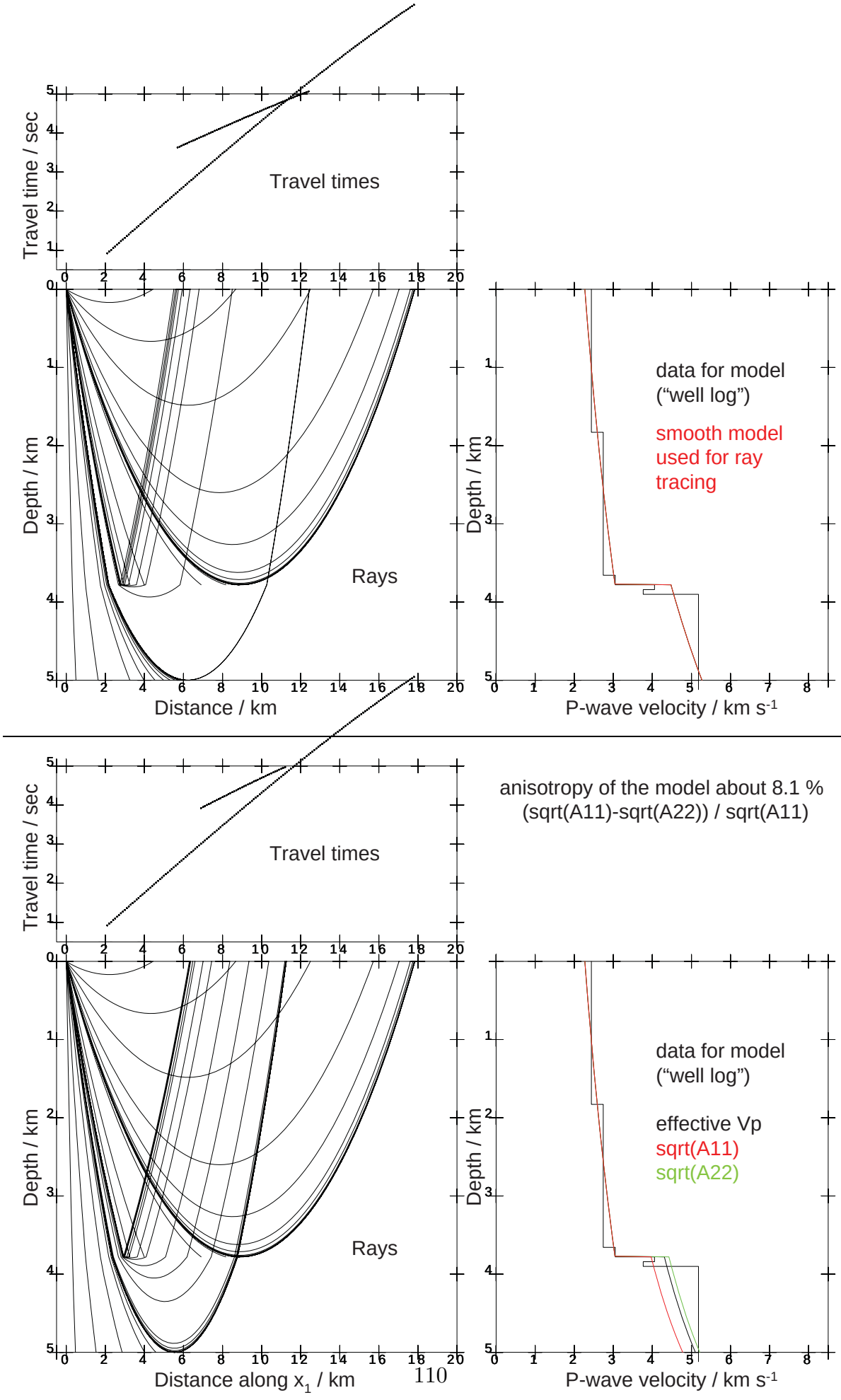

Figure 6: *Top:* isotropic model 2. *Bottom:* anisotropic model 4.

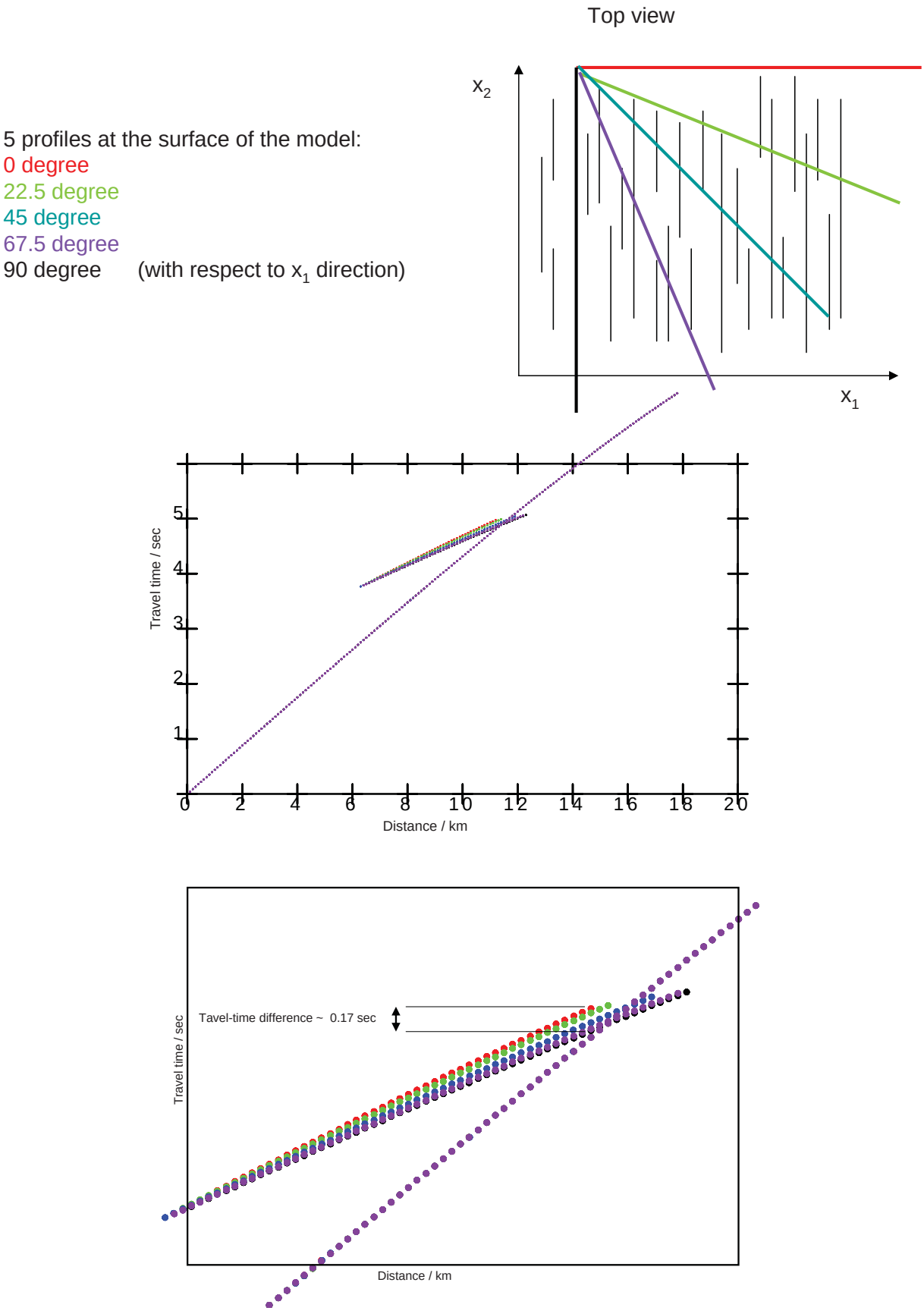

Figure 7: *Top:* a sketch of 5 profiles at the surface of the model. *Middle:* travel–time curves along the profiles in the anisotropic model 4. *Bottom:* a detail of the travel–time curves.

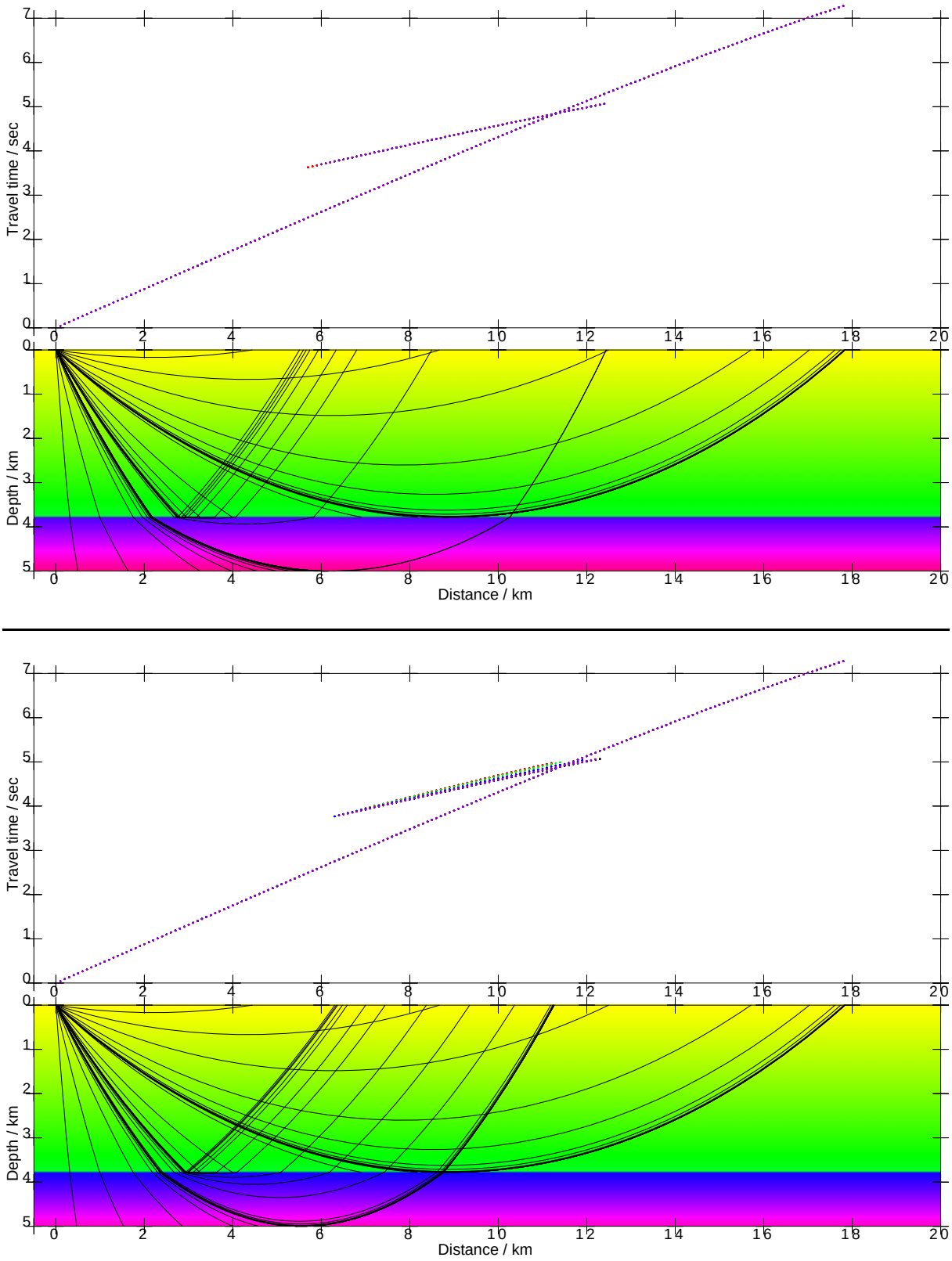

Figure 8: *Top:* P-wave $x_1 - x_3$ velocity section in the isotropic model 2 plotted together with the rays traced in the $x_1 - x_3$ plane, and together with the travel–time curves for the 5 profiles shown in Figures 5 and 7. (The figure shows the same information as Figure 6, but in different graphical form.) *Bottom:* anisotropic model 4. (The figure shows the same information as Figures 6 and 7, but in different graphical form.)

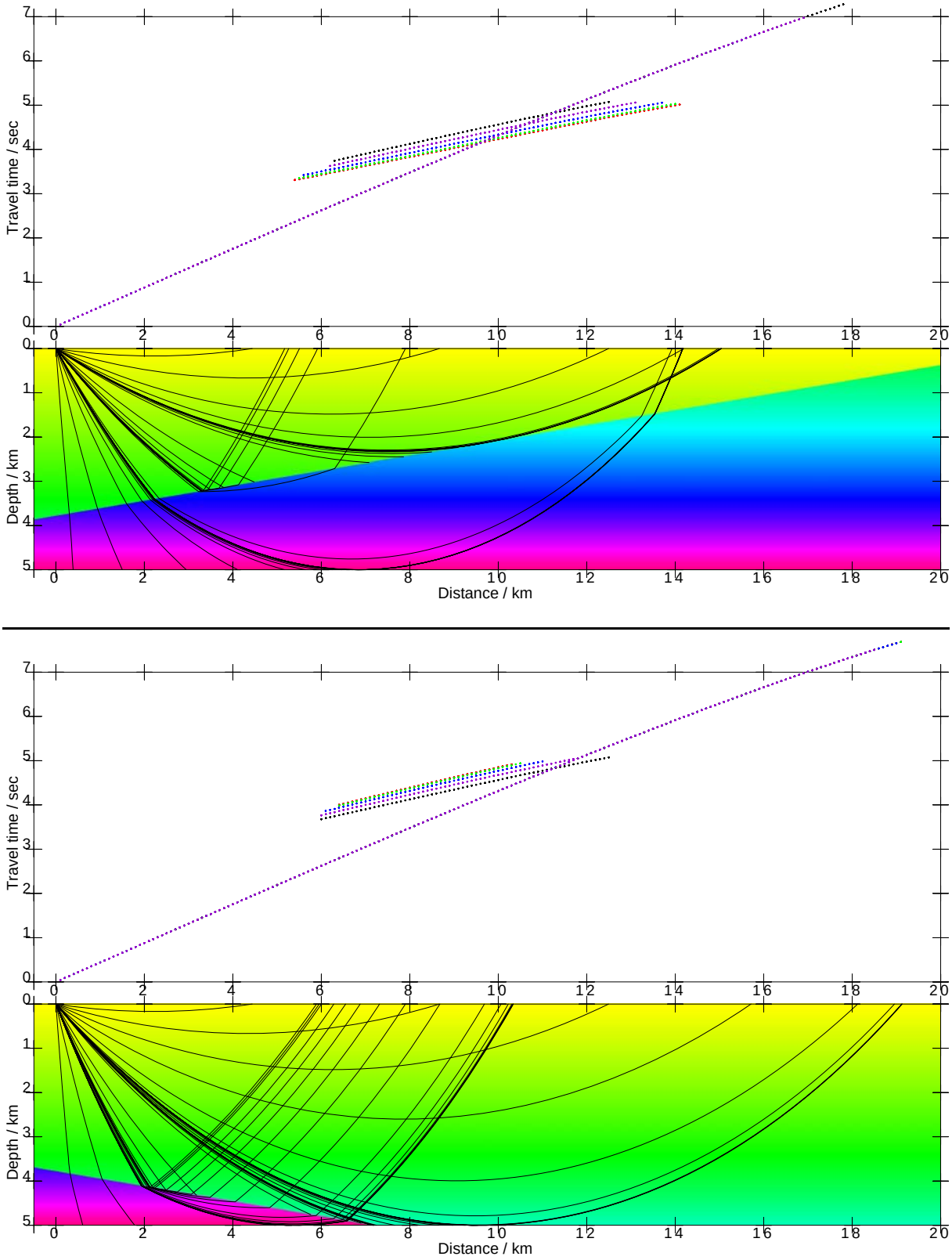

Figure 9: *Top:* 2.5-D isotropic model with the same depth dependance of the velocity as in the isotropic model 2, but the structural interface is inclined with respect to the source. *Bottom:* structural interface declined away from the source.

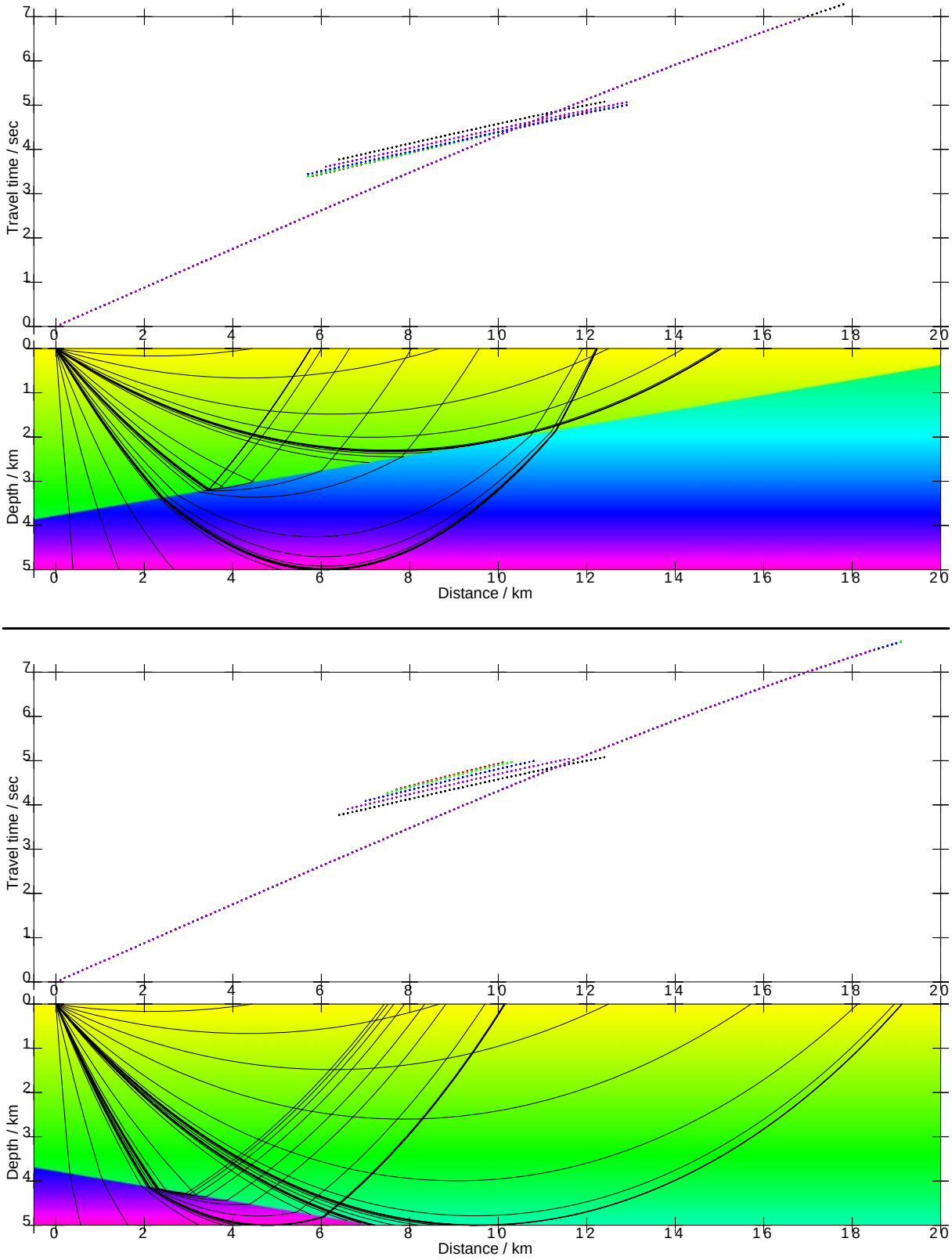

Figure 10: *Top:* 2.5-D anisotropic model with the same depth dependance of the velocity as in the anisotropic model 4, but the structural interface is inclined with respect to the source. *Bottom:* structural interface declined away from the source.

2.4 Models with VTI anisotropy

Our next task was to examine the effects of vertical cracks in case of a medium with VTI anisotropy. We construct anisotropic model 5 which is derived from isotropic model 2 by including vertical anisotropy of approximately 10% to the lower layer, see the top panels of Figure 11. We then add vertical cracks to the anisotropic layer and thus construct anisotropic model 6, see the bottom panels of Figure 11. Figure 12 than shows that the effects of vertical cracks on the model with VTI layer are very similar to the effect of vertical cracks on the model with isotropic layer, compare Figure 12 with Figure 8.

2.5 Models with low velocity layers

The last class of the examined models were isotropic models derived from isotropic model 2 by including three different low-velocity layers. Isotropic model 3 has a thin low-velocity channel, isotropic model 4 has a thin layer of a very low velocity, see Figure 13. Isotropic model 5 has a thicker layer of a very low velocity, and isotropic model 6 contains low-velocity halfspace, see Figure 15. Figures 14 and 16 show the effects of low-velocity channels on the travel–time curves. We see that the effects of thin low-velocity layer are almost invisible, they start to be visible in the case of thin layer of a very low velocity, and they are clearly visible in the case of a thicker layer of a very low velocity. We can also see that the low velocity channels slow down the affected part of the travel–time curves, but they do not influence the shape of the travel–time curves and do not result in any qualitative changes of the travel–time curves which would enable to clearly identify the low velocity channels from the measured travel–time curves. Only in the unrealistic case of low-velocity halfspace the travel–time curve differs considerably, but this is rather the result of missing high velocities in the lower part of the model, than of the low-velocity halfspace itself.

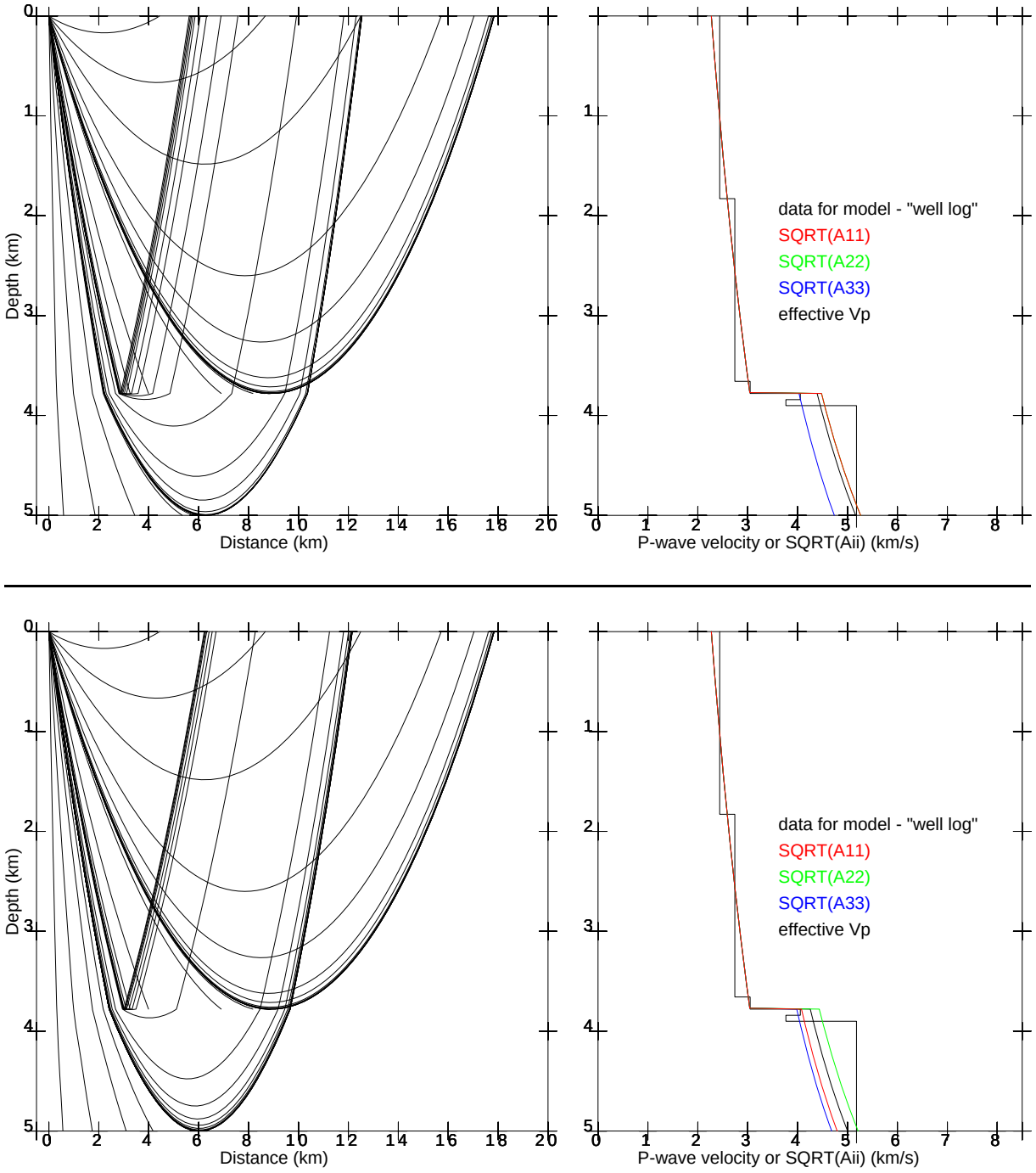

Figure 11: *Top:* anisotropic model 5 has lower layer with VTI anisotropy of approximately 10 %. *Bottom:* anisotropic model 6 has lower layer with vertical anisotropy about 10 % and horizontal anisotropy about 8 %, which simulates VTI medium with vertical cracks in the $x_2 - x_3$ plane.

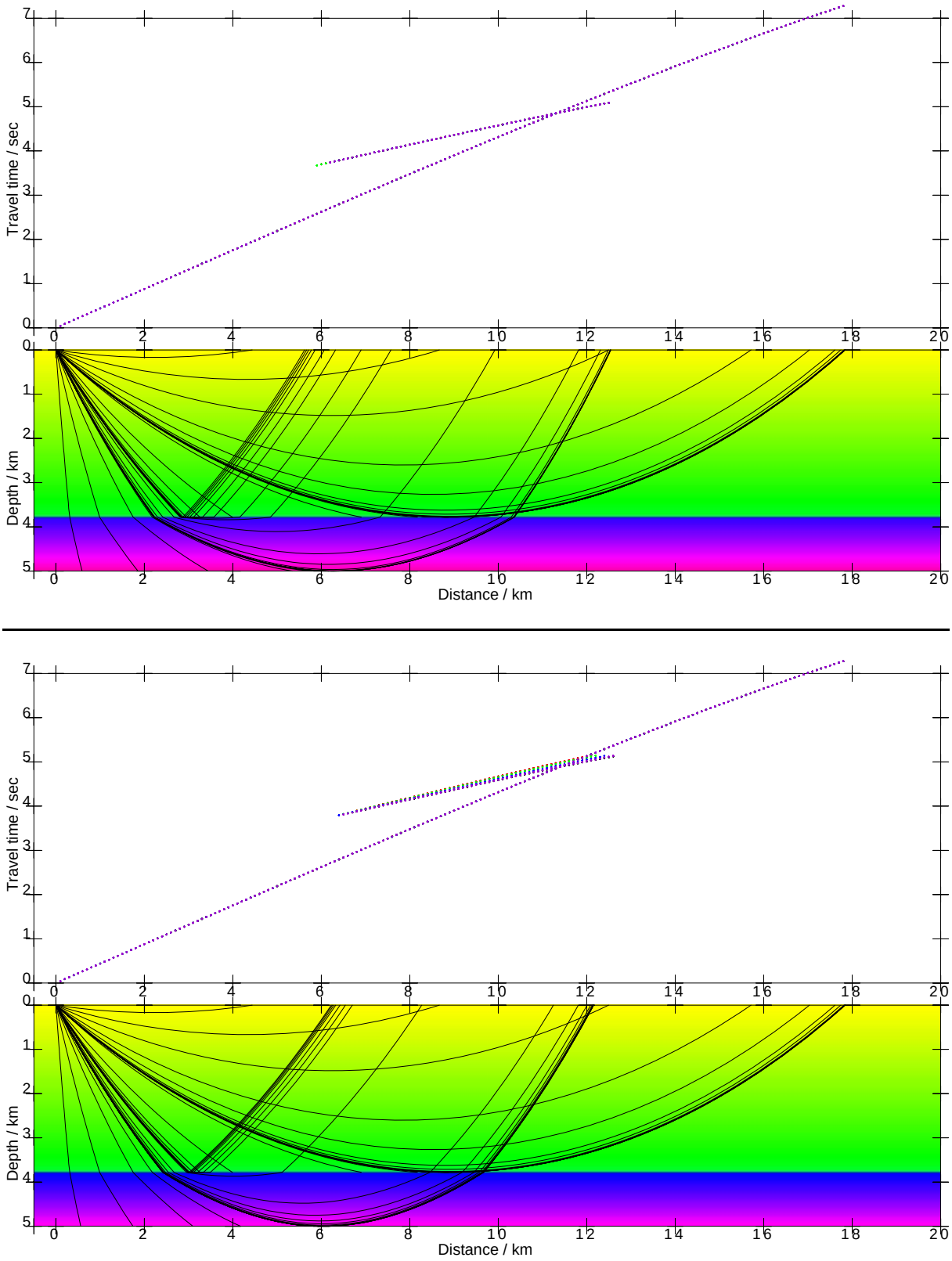

Figure 12: *Top:* anisotropic model 5 with lower layer with VTI anisotropy of approximately 10 %. *Bottom:* anisotropic model 6 with lower layer with vertical anisotropy about 10 % and horizontal anisotropy about 8 %, which simulates VTI medium with vertical cracks in the $x_2 - x_3$ plane.

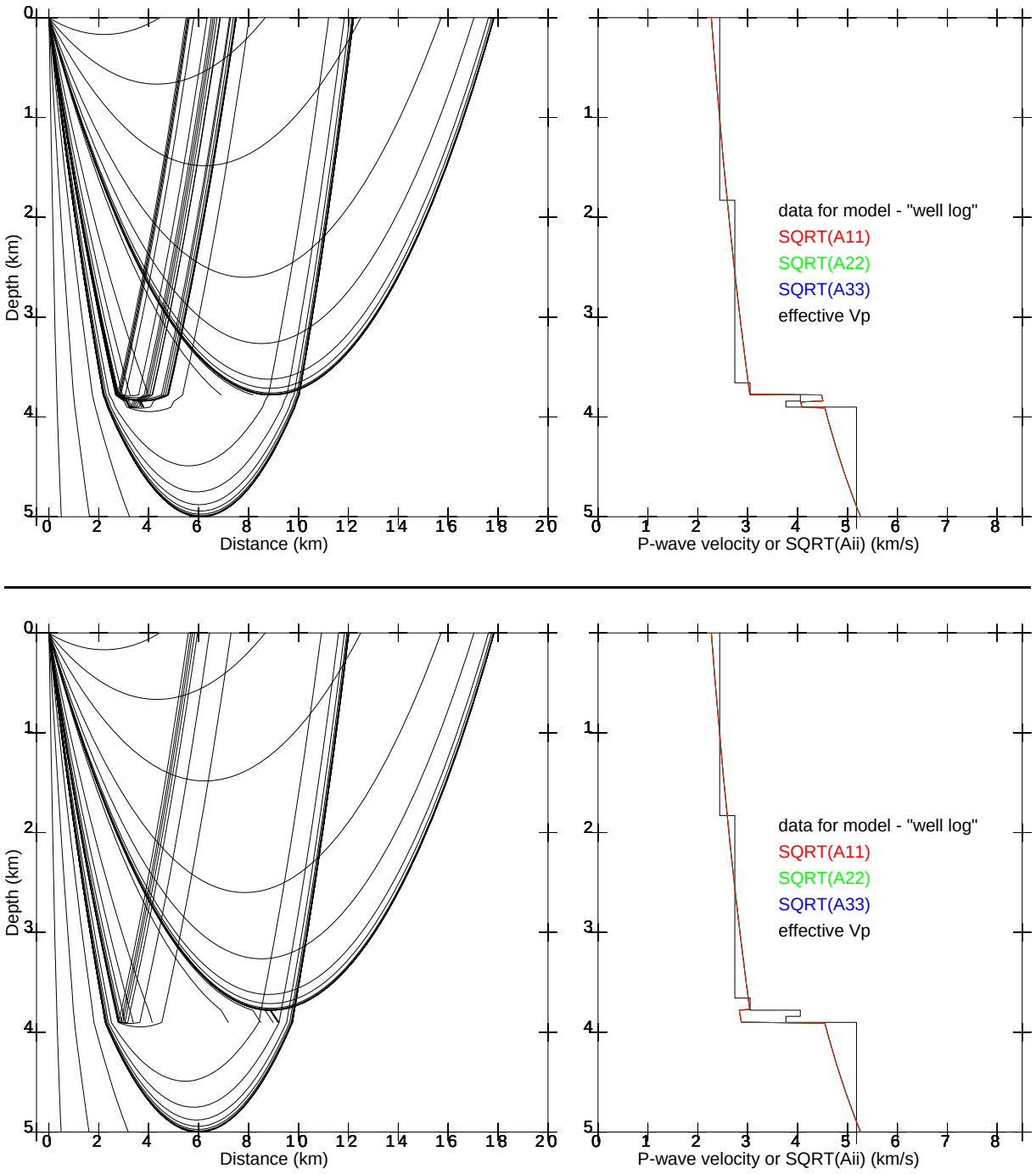

Figure 13: *Top:* isotropic model 3 with a thin low-velocity channel. *Bottom:* isotropic model 4 with thin layer of a very low velocity.

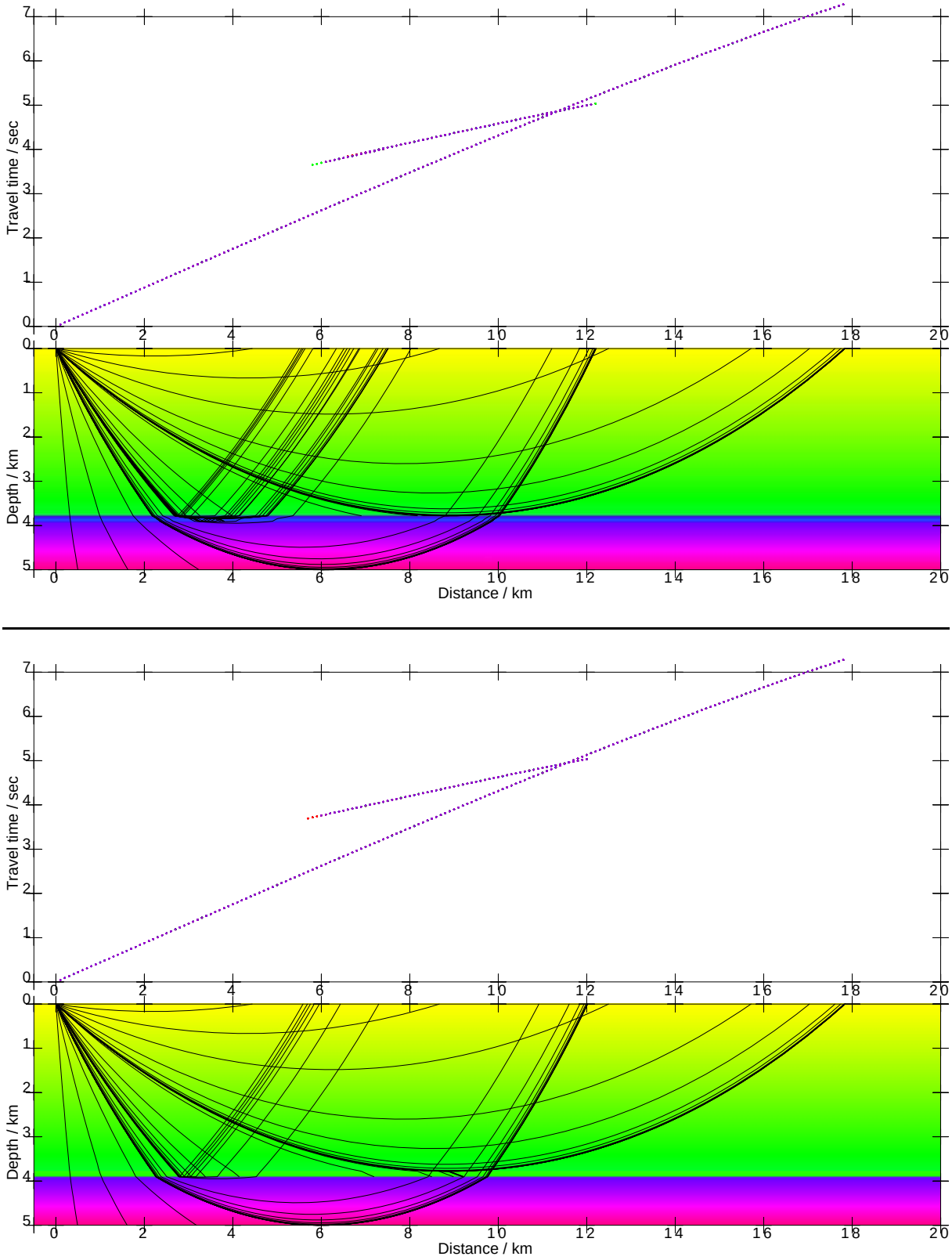

Figure 14: *Top:* isotropic model 3 with a thin low-velocity channel. *Bottom:* isotropic model 4 with thin layer of a very low velocity.

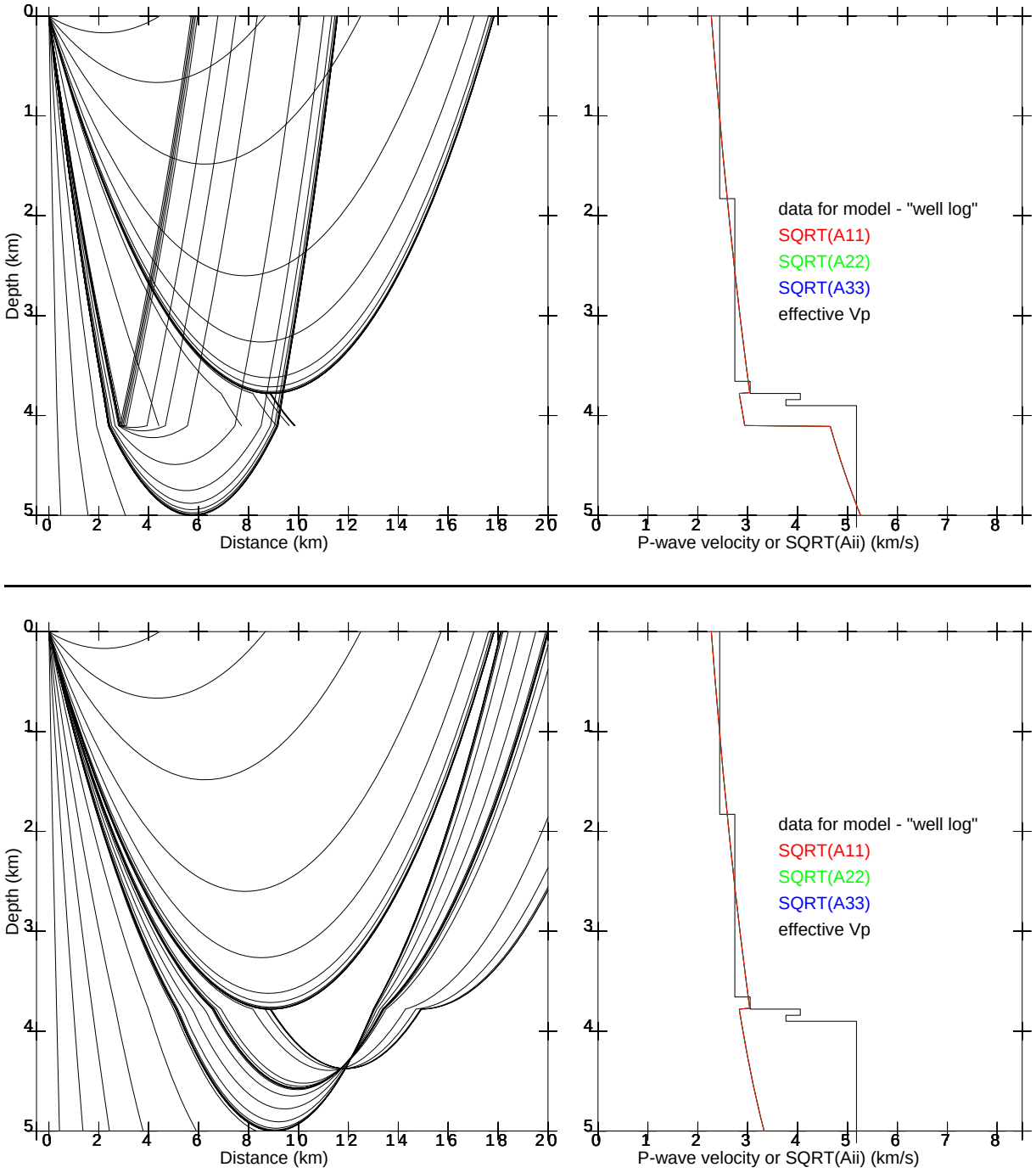

Figure 15: *Top:* isotropic model 5 with thick layer of a very low velocity. *Bottom:* isotropic model 6 with low-velocity halfspace.

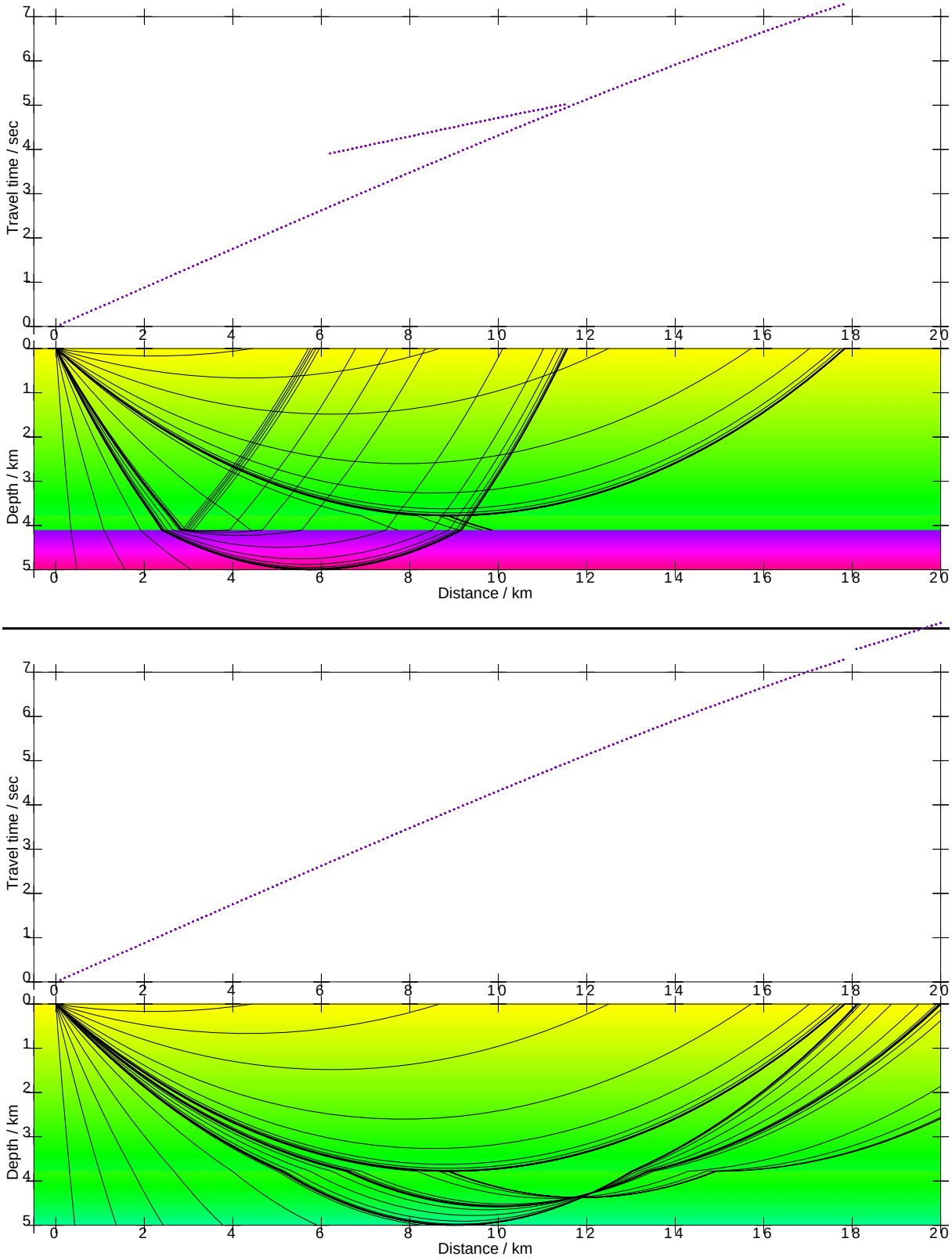

Figure 16: *Top:* isotropic model 5 with thick layer of a very low velocity. *Bottom:* isotropic model 6 with low-velocity halfspace.

Conclusions

In the models considered in this study, the effects of the vertical cracks on the P-wave travel–time curves start to be visible from the anisotropy of 7.5%. The vertical cracks slow down the rays propagating perpendicularly to the cracks, while their influence on the rays propagating parallel to the cracks is negligible. This effect appears similarly either when we introduce vertical cracks to the isotropic layer, or when we introduce them to the VTI layer. Structural interface declined away from the source in the isotropic model has similar effects on the travel–time curves as the vertical cracks, while the interface inclined towards the source has opposite effects. Effects of dipping interface and of vertical cracks sum up. Low-velocity channels slow down the affected part of the travel–time curve, but do not produce any qualitative effects which would enable to identify them from the travel–time curves.

Acknowledgements

I am grateful to Leo Eisner who motivated me to perform this study and came with many ideas regarding which models should be investigated.

The research has been supported by the Grant Agency of the Czech Republic under contracts 16-01312S and 16-05237S, truecm by the Ministry of Education, Youth and Sports of the Czech Republic within research project CzechGeo/EPOS LM2015079, and by the members of the consortium "Seismic Waves in Complex 3–D Structures" (see "http://sw3d.cz").

References

Bulant, P. (2002): Sobolev scalar products in the construction of velocity models — application to model Hess and to SEG/EAGE Salt Model. *Pure appl. Geophys.*, **159**, 1487–1506, online at "http://sw3d.cz".

Bulant, P. & Klimeš, L. (1999): Interpolation of ray theory traveltimes within ray cells. *Geophys. J. int.*, **139**, 273–282, online at "http://sw3d.cz".

Grechka, V. (2009): *Applications of Seismic Anisotropy in the Oil and Gas Industry.* EAGE, Houten, The Netherlands, ISBN 978-90-73781-68-9.

Schoenberk, M. & Sayers, C. (1995): Seismic anisotropy of fractured rock. *Geophysics*, **60**, 204–211.